P. Lalor, H. Sehitoglu,* and R. C. McClung**

Mechanics Aspects of Small Crack Growth from Notches – the Role of Crack Closure

REFERENCE Lalor, P., Sehitoglu, H., and McClung, R. C., **Mechanics Aspects of Small Crack Growth from Notches – the Role of Crack Closure**, *The Behaviour of Short Fatigue Cracks*, EGF Pub. 1 (Edited by K. J. Miller and E. R. de los Rios) 1986, Mechanical Engineering Publications, London, pp. 369–386.

ABSTRACT The concept of fatigue crack closure has come to be one of the most effective tools in explaining the anomalous propagation behaviour of small cracks. A two-dimensional, plane stress, elasto-plastic finite element model is employed to predict the opening and closure behaviour of small fatigue cracks emanating from blunt notches. The model incorporates changing boundary conditions associated with the intermittent contact and separation of the crack faces and allows cyclic crack extension through the mesh. Crack opening and closure levels, near crack stress fields, and crack tip plastic zone sizes are determined as a function of crack length. The model predicts crack opening and closure levels to increase and then stabilize as the crack grows away from the notch. The influence of load level on small crack closure behaviour is also considered. Predictions correlate with, and give insight to, experimental results.

Nomenclature

c	Half notch width
$d\mu$	Scalar used in Ziegler's rule
E	Modulus of elasticity
$\dot{\epsilon}^{p}_{ij}$	Plastic strain rate tensor
E_p	Plastic modulus
f	von Mises yield function
k	Stiffness of truss element
K	Stress intensity factor
K_{min}, K_{max}	Minimum and maximum stress intensity
ΔK, ΔK_{eff}	Range in stress intensity factor, and effective stress intensity factor
l	Crack length measured from the notch
l/c	Crack length normalized by half notch width
R	Stress ratio, minimum stress/maximum stress
r_p	Notch plastic zone size
S, ΔS	Applied stress level and stress range
S_a, S_{max}	Stress amplitude and maximum applied stress level
S_{clos}, S_{open}	Applied stress level at crack closure and at crack opening
S_{ij}, S^{c}_{ij}	Deviatoric stress and back stress tensor
w, Δw	Maximum plastic and reversed plastic zone size
x,y	Coordinate axes at crack tip
X, Y	Global coordinate axes located at the centre of notch (FEM)

* Department of Mechanical and Industrial Engineering, University of Illinois at Urbana-Champaign, 1206 West Green Street, Urbana IL 61801, USA.

σ_o	Yield stress in tension
σ_{ij}	Stress tensor
σ_{yy}	y component of local (notch and/or crack tip) stress
δ_{ij}	Kronecker delta (identity tensor)

Introduction

It is now well known that a crack may be closed during a significant portion of a fatigue cycle (1). This crack closure is a result of the plastically deformed material ahead of the crack tip and is most significant under plane stress conditions. As the crack extends, this material is unloaded and forms residual displacements on the crack surfaces. These residual displacements cause the crack surfaces to contact earlier than expected during unloading. Once contact is attained, further unloading results in residual compressive stresses in the wake of the crack tip. In order for the crack to re-open, these stresses must be overcome by the applied load. Based on experimental and analytical results (2)(3), it is expected that crack opening and closure levels approach a steady-state value with increasing crack length. However, a majority of a component's fatigue life may well be consumed in the small crack growth regime where opening and closure levels are continuously changing. It is, therefore, desirable to understand the influence of load level, geometry, crack length, and material microstructure on the behaviour of these small cracks. The effects of crack length and applied load on opening and closure levels are addressed in this study.

Analytical studies (4)–(6) based on assumed residual displacement fields have been performed to predict crack opening loads. Estimates of the compressive residual stresses behind the crack at minimum load have been used to establish the crack opening loads necessary to overcome them. These models were based on the Dugdale (strip-yield) model (7) modified to leave plastically deformed material in the wake of the advancing crack. Many assumptions are inherent in these analytical methods.

For physically small cracks, especially small cracks growing in the vicinity of a notch plastic zone where plastic zone size is not small compared to crack size, linear elastic fracture mechanics (LEFM) concepts fall short in characterizing crack tip stress–strain behaviour. Finite element methods (FEM) have been applied to crack closure studies to account for both notch and crack tip plasticity (8)–(10). Elasto-plastic material behaviour and geometry can be accurately accounted for with finite element methods. In the present work, small fatigue crack growth from a blunt notch (circular hole) is modeled with FEM and the results are compared to analytical and experimental studies performed by Sehitoglu (2)(3). Near crack stress fields determined from the FEM study add much support to the understanding of small crack growth behaviour.

Several factors thought to influence small crack growth behaviour are not included in the present work. Grain size is critical to small crack growth since deceleration and non-propagation of small cracks may be attributed to blockage of slip by the grain boundaries (11). In the present work the crack was allowed to grow perpendicular to the principal stress direction with no effect of shear loading on crack surfaces. Specifically, tortuosity of the crack path observed near the threshold region may influence crack growth rates. The crack growth rate behaviour reported here, however, is considered to be outside the regime in question.

The purpose of the present study is to:

(a) simulate the crack opening and closure behaviour of the 1070 steel using elasto-plastic finite element methods. (This is the steel used in previously reported experimental studies (2)(3).)
(b) determine stress (including residual stress) fields in the vicinity of growing cracks;
(c) analyse the influence of the notch inelastic field on crack closure;
(d) determine the influence of crack length and applied load level on crack opening and closure levels and compare the results with experiments (2)(3).

Analysis

A small fatigue crack growing in a notched plate (Fig. 1) subjected to completely reversed ($R = -1$) cyclic loading is analysed here. The mesh is composed of four-noded isoparametric quadrilateral elements with a 2×2 integration rule. Nodal coordinates are updated after application of each load increment. Material properties incorporated in the model were those of a 1070 wheel steel (class U). Experimental results on this material are tabulated in references (2) and (3). A replica technique with a scanning electron microscope has been used to determine crack tip opening and closure levels in these references. The stress–strain curve of the material is shown in Fig. 2. Monotonic and cyclic curves at 20°C coincide for this material.

The plasticity theory incorporated in the model employs a von Mises yield surface and uses Ziegler's modification to Prager's hardening rule (12) for translation of the yield surface. This hardening rule was chosen to account for the material anisotropy (Bauschinger effect) associated with reversed yielding (kinematic hardening) in the vicinity of a fatigue crack. The von Mises yield condition is given by (repeated indices imply summation)

$$f = \tfrac{3}{2}(S_{ij} - S_{ij}^c)(S_{ij} - S_{ij}^c) - \sigma_o^2 = 0 \qquad (1)$$

where σ_o is the yield stress in tension and S_{ij} are the stress deviators

$$S_{ij} = \sigma_{ij} - \tfrac{1}{3}\delta_{ij}\sigma_{kk} \qquad (2)$$

S_{ij}^c represents the total translation of the centre of the yield surface in deviatoric stress space due to work hardening and is often termed the deviatoric back

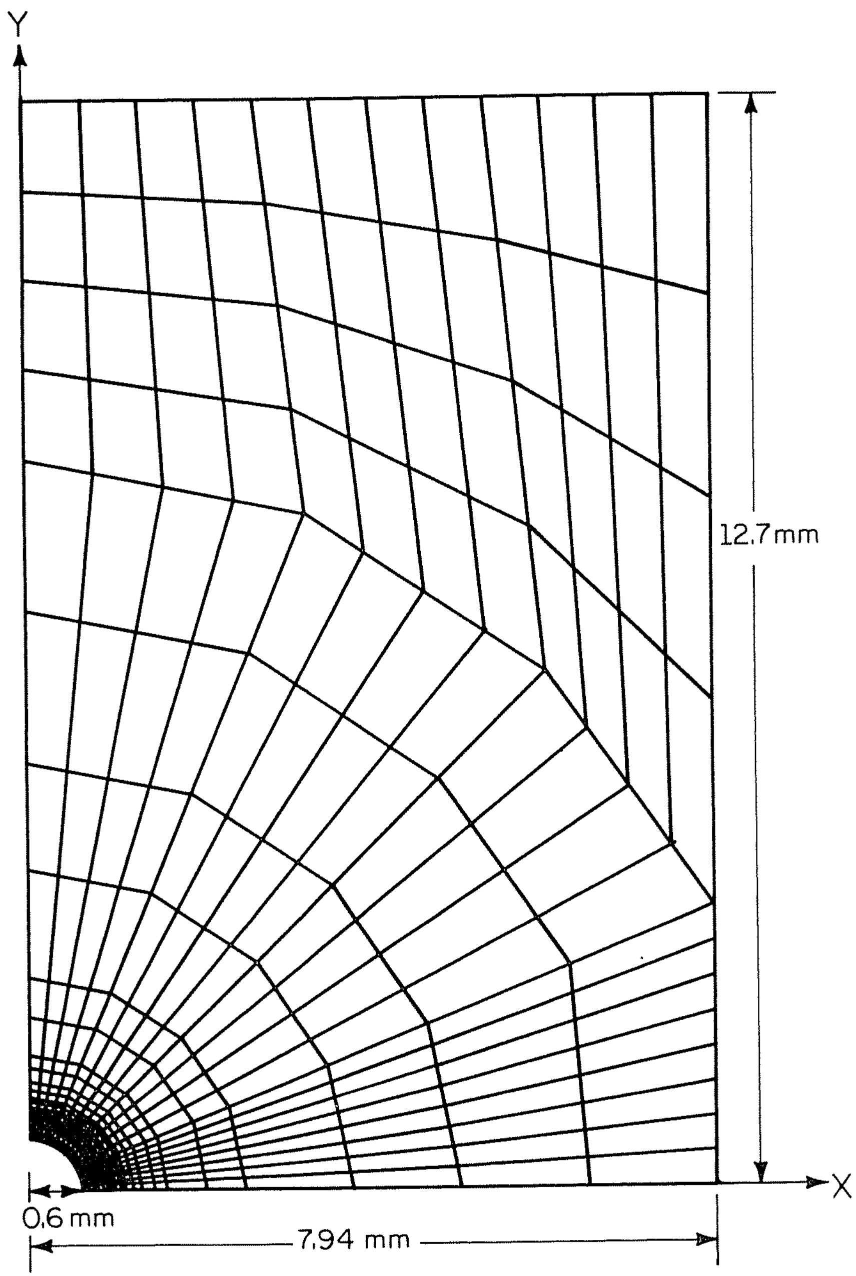

Fig 1 Element mesh for centre notched member

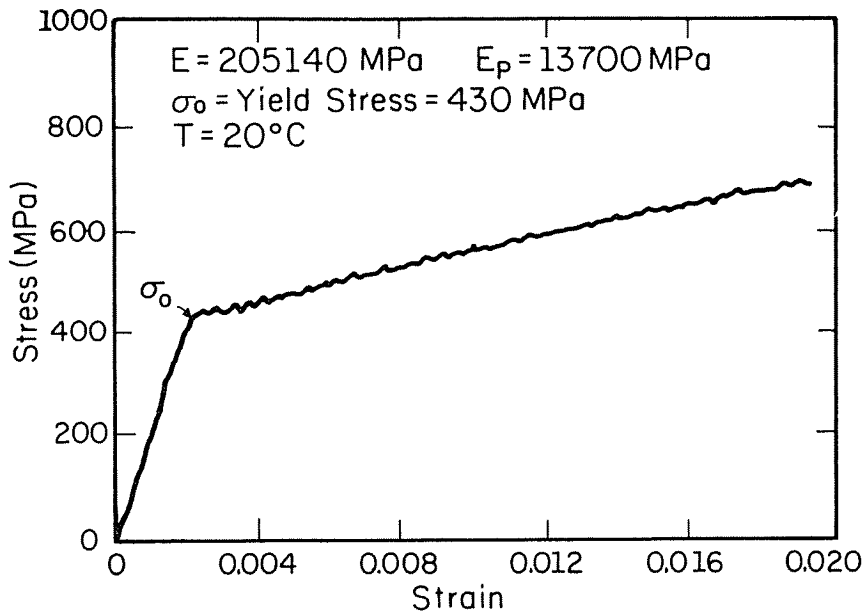

Fig 2 Experimental stress–strain relation for 1070 wheel steel (Class U)

stress tensor. The flow rule and Ziegler's kinematic hardening rule are represented, respectively, by

$$\dot{\epsilon}^{p}_{ij} = G \frac{\partial f}{\partial S_{ij}} \frac{\partial f}{\partial S_{kl}} \dot{S}_{kl} \tag{3}$$

and

$$\dot{S}^{c}_{ij} = d\mu(S_{ij} - S^{c}_{ij}) \tag{4}$$

Here, G is a scalar (constant) and $d\mu$ is a scalar determined from the consistency condition df = 0. The term $\dot{\epsilon}^{p}_{ij}$ represents increments of the plastic strain tensor. A state of plane stress is modeled and for simplicity a bilinear representation of the stress–strain curve is used. This simplification is reasonable for the material of interest (Fig. 2). The yield stress, σ_o, is 430 MPa.

The procedure which permits cyclic crack extension and variable boundary conditions associated with the intermittent contact and separation of the crack surfaces during the loading history is illustrated in Fig. 3. Truss elements of variable stiffness are attached to the nodes along the crack face. The stiffness of a truss is set to an extremely high value ($k \rightarrow \infty$) when that portion of the crack is closed. When a portion of the crack satisfies the condition for opening, the stiffness of the associated truss is set to zero ($k = 0$) thus allowing the crack to open. (Note that the crack surfaces are free to move in the x direction.)

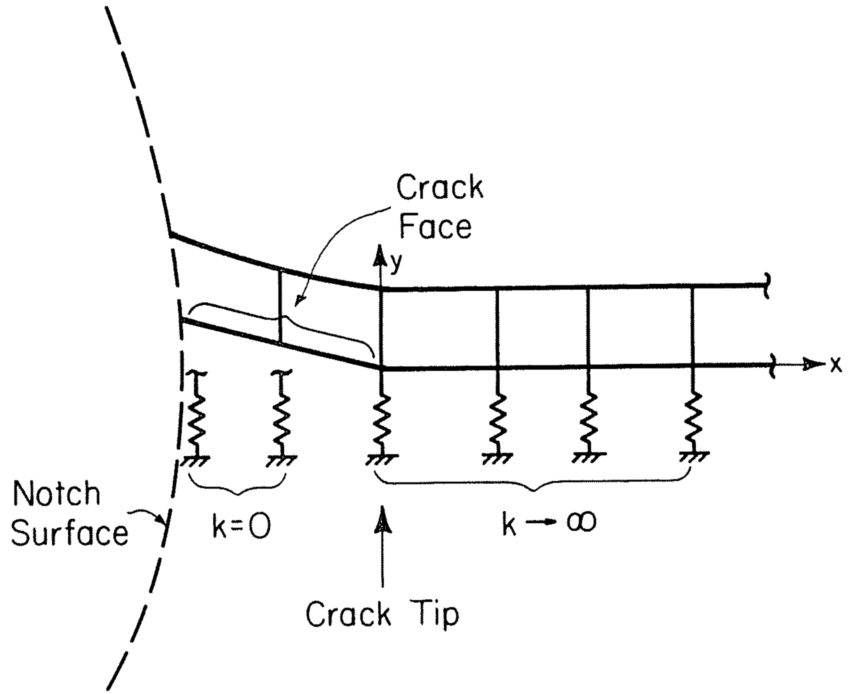

Fig 3 Representation of control of boundary conditions along the crack face

In other studies (**8**) of crack closure using the finite element method, a section of crack was permitted to open ($k = 0$) when the applied loading caused the y displacement of that node along the crack surface to become positive. This displacement appears to be dependent on the finite stiffness value assigned to the spring holding the crack surface closed. Although most results showed good agreement with experiments, this criterion gave closure levels higher than opening levels, which does not correspond to experimental results (**2**)(**3**).

The criteria for crack opening implemented in this study provides the correct trends in opening and closure levels. It has been postulated that in order for a fatigue crack to open, the applied loading must overcome the compressive residual stresses left in the wake of the crack tip (**1**). Here, the σ_{yy} components in the crack surface elements are monitored throughout the loading portion of the history. When σ_{yy} for a crack surface material point changes from compressive to zero to slightly tensile, the stiffness of the associated truss element is changed to zero, thereby allowing that portion of the crack to open. Crack opening level, S_{open}, is defined as the applied load level that overcomes all compressive residual stresses in the wake of the crack tip. At this time, crack propagation is once again assumed to be possible.

A section of crack is said to be closed ($k \rightarrow \infty$) when the y component of the coordinates of the particular node being considered along the crack face returns to its original ($y = 0$) position. These nodal coordinates are monitored throughout the unloading portion of the history. In this study, crack closure level, S_{clos}, is defined as the applied load level at which the node directly behind the crack tip first closes thus eliminating the possibility of further crack propagation. Similarly, the first contact of the crack tip region has been defined as the experimental S_{clos}. An alternate definition of S_{clos} based on complete closure of the crack surfaces is also possible but yields S_{clos} levels which are lower than the above case.

Crack extension is achieved by arbitrarily choosing to release the present crack tip node ($k = 0$) when the peak of each load cycle is reached. Upon doing so, the load is redistributed and the new crack tip is located in front of the node just released. The increment of crack extension is thus equal to the side length of a crack surface element (0.028 mm). Presently, this crack extension criteria is arbitrary but could readily be modified to represent a crack-growth law based on, for instance, crack tip opening displacements.

The procedure described above was implemented to propagate a small fatigue crack from initiation ($l/c = 0$) well into the region of long crack behaviour ($l/c = 1.5$) where $c = 0.6$ mm (half notch width). The crack grew out of the notch in a plate (Fig. 1) subjected to $R = -1$ loading with an applied stress amplitude of $S_a = 207$ MPa. Then, the case of $S_a = 310$ MPa was considered. In order to reduce computation time, the crack length was extended by two element side lengths in the fine region of the mesh or by one element side length in the coarser region of the mesh at the top of each load cycle. The crack growth increment was then 0.056 mm per cycle. If a slightly larger or smaller increment in crack extension per cycle were used, the results for the same total crack lengths were not affected provided that the increment of crack extension did not exceed the size of the crack tip plastic zone.

The loading was carried out in small increments in order to monitor the crack surface elements stresses and nodal coordinates as criteria for determining opening and closure levels. Plots of numerical results are superimposed on experimental results where applicable.

Results

Crack opening and closure levels, S_{open} and S_{clos}, determined with FEM, are plotted as a function of normalized crack length in Fig. 4. These results are indicated with symbols F* and F, respectively. Results consistently indicate crack opening levels to be higher than closure levels. There exists a favourable agreement among opening and closure levels obtained with the experimental (Exp.) and analytical methods (A*, A) shown in Fig. 4. Note that closure levels predicted by FEM compare better with experimental values than did the closure levels predicted by the analytical method (based on the Dugdale model)

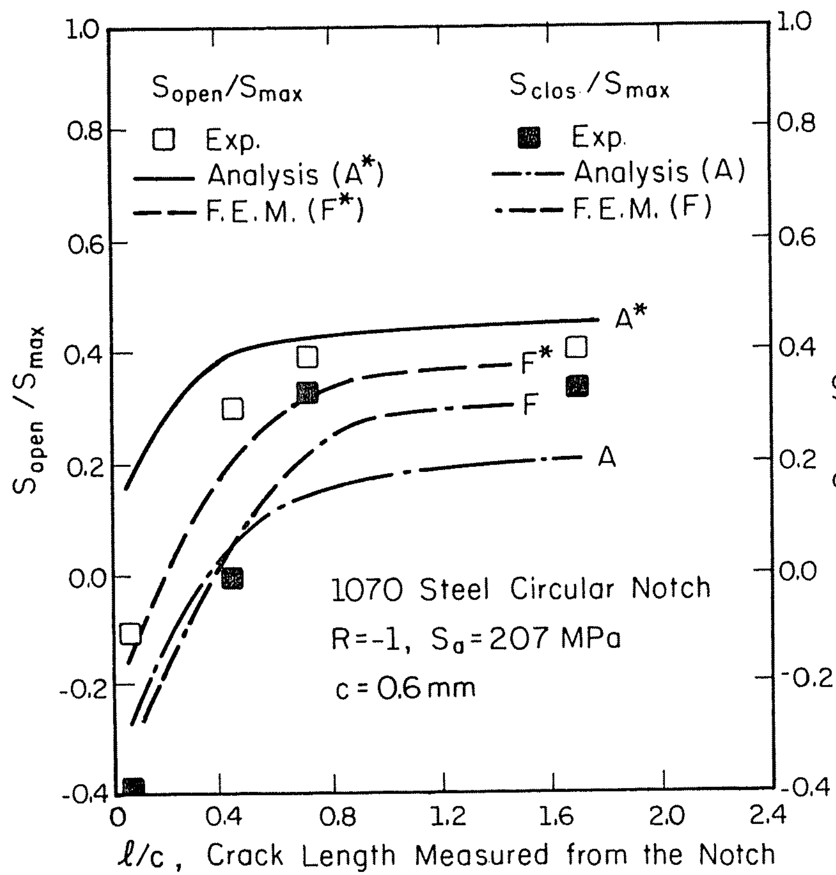

Fig 4 **Three different techniques to determine crack opening and closure levels for a crack growing from a circular notch**

This difference is due to the fact that both the experimental and the FEM techniques considered closure at the crack tip but the analytical closure levels were calculated based on closure over the entire crack length (**2**). The experimental crack opening and closure results were obtained by a replicating technique and viewing the replicas in the scanning electron microscope (**3**).

The effective stress range during which the crack is open and capable of propagating is defined as

$$\Delta SK_{eff} = S_{max} - S_{open} \tag{5}$$

The corresponding effective stress intensity range, ΔK_{eff}, has been used to intepret crack growth rate behaviour (**1**)–(**3**). In Fig. 5, ΔK_{eff} is used to indicate that changing crack opening level with increasing crack length and its influence

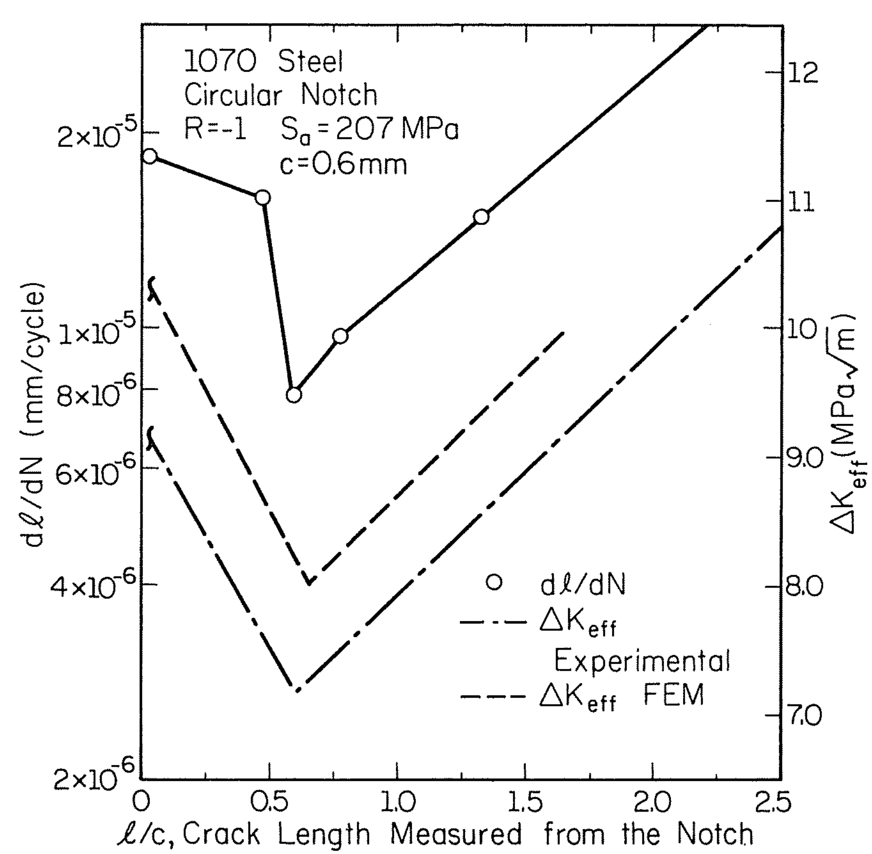

Fig 5 **Changing effective stress intensity range as a function of crack length and its influence on crack growth rate**

on the experimentally measured crack growth rate. In this case ΔK_{eff} was computed using ΔK (equations (5a) and (5b) of reference (**2**) modified with experimental and FEM opening levels (S_{open}), respectively. The experimentally and numerically (FEM) computed ΔK_{eff} levels agree within 10 per cent for most cases. Crack growth rates are seen to decrease with increasing crack length then increase again. Closure effects appear to account for this behaviour as shown in Fig. 5; note that the ΔK_{eff} curves in Fig. 5 are not extended to $\Delta K_{eff} = 0$.

Use of the finite element method in modelling fatigue crack growth problems gives access to some parameters that are not as readily obtained with other methods. Two of these parameters, near crack stress fields and crack tip plastic zones for the hardening material considered, are discussed below.

Figure 6 presents plots of the near tip stress fields for different crack lengths.

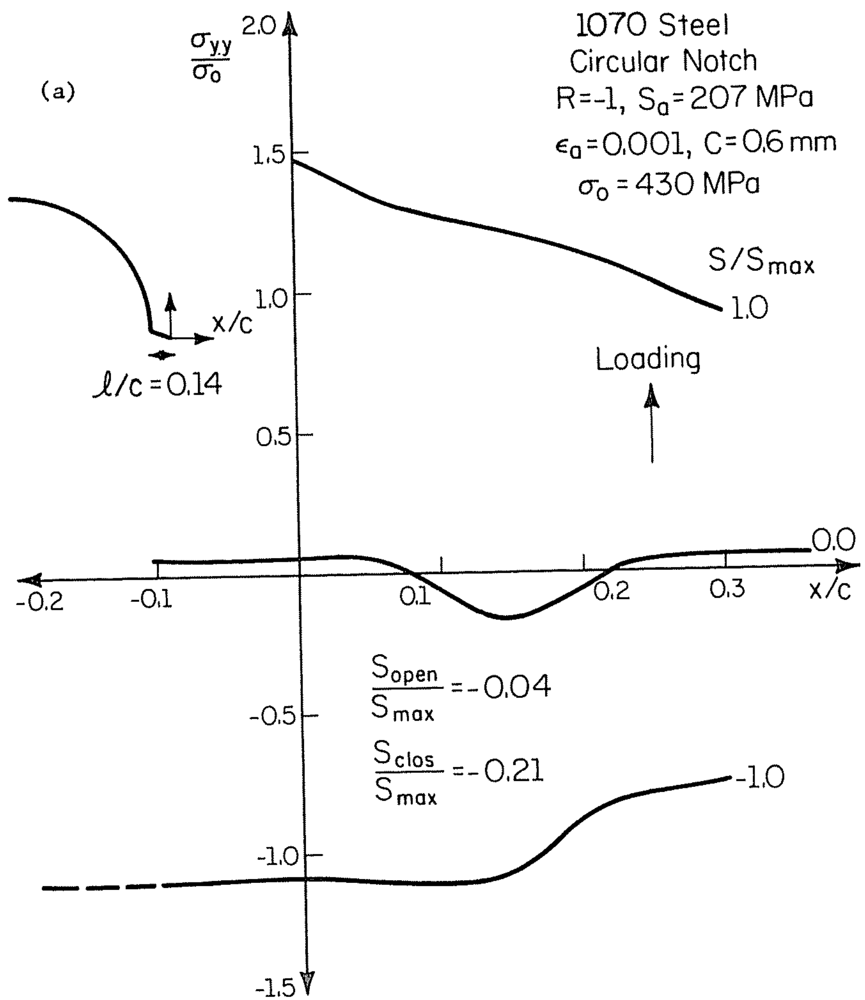

Fig 6 Near crack stress fields during different stages of loading
(a) $l/c = 0.14$ (b) $l/c = 0.6$ (c) $l/c = 0.8$

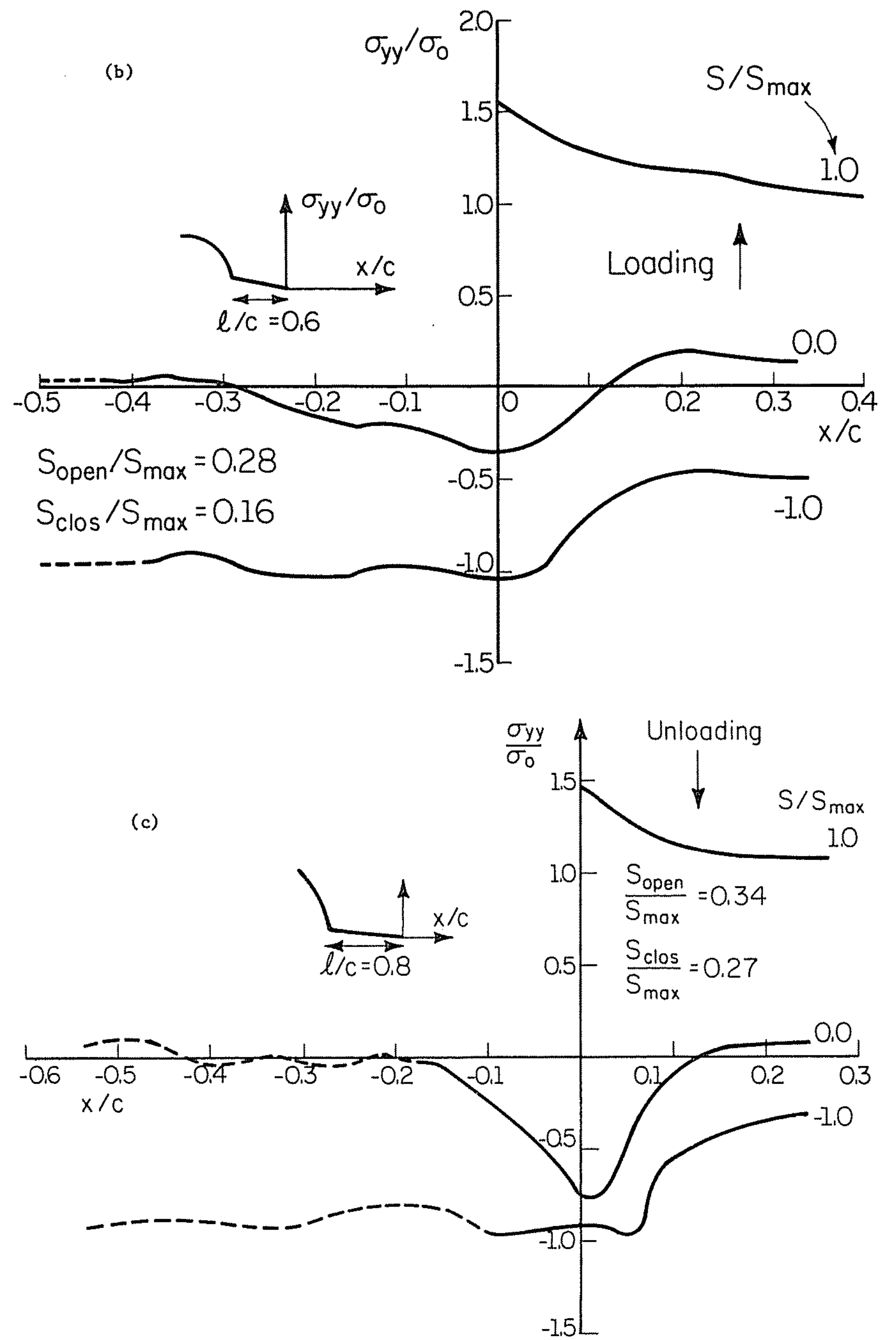

Three different stress fields are plotted on each curve representing different stages of the cycle; loading in Fig. 6(a) and (b), unloading in Fig. 6(c). The vertical axis is the stress field in the y direction normalized by the uniaxial yield stress, σ_o. On the horizontal axis, the location $x/c = 0$ denotes the crack tip; the position $x/c = -l/c$ corresponds to the notch surface. The shorter crack (Fig. 6(a)) is open during a larger portion of a loading cycle than the longer crack in Fig. 6(b). This occurs due to the extent of closure as a function of crack length. Note that due to the influence of the notch stress field, the magnitudes of the compressive residual stresses at minimum load ($S/S_{max} = -1.0$) are approximately equal for both crack lengths. Stress fields for a fatigue crack during different stages of the unloading portion of a cycle are shown in Fig. 6(c). The onset and evolution of the compressive residual stresses in the wake of the crack tip can be seen after contact of the crack surfaces is observed.

The stress fields created by the presence of the notch also appear to affect small crack behaviour (**13**)–(**15**). The uncracked notch root material stress–strain response is shown in Fig. 7 to indicate the plastic strain field the small

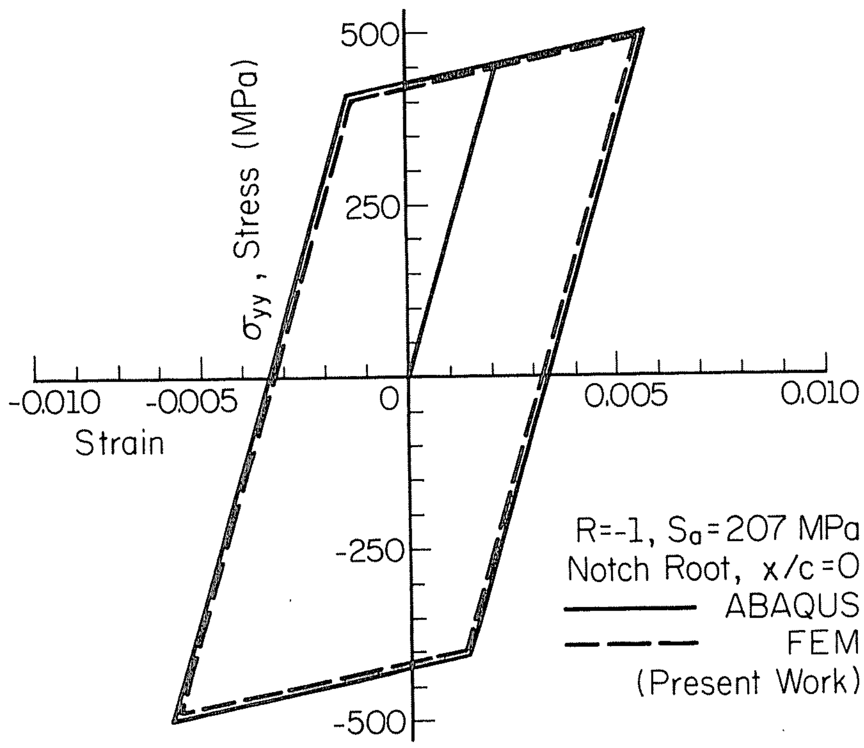

Fig 7 Stress–strain response at uncracked notch root

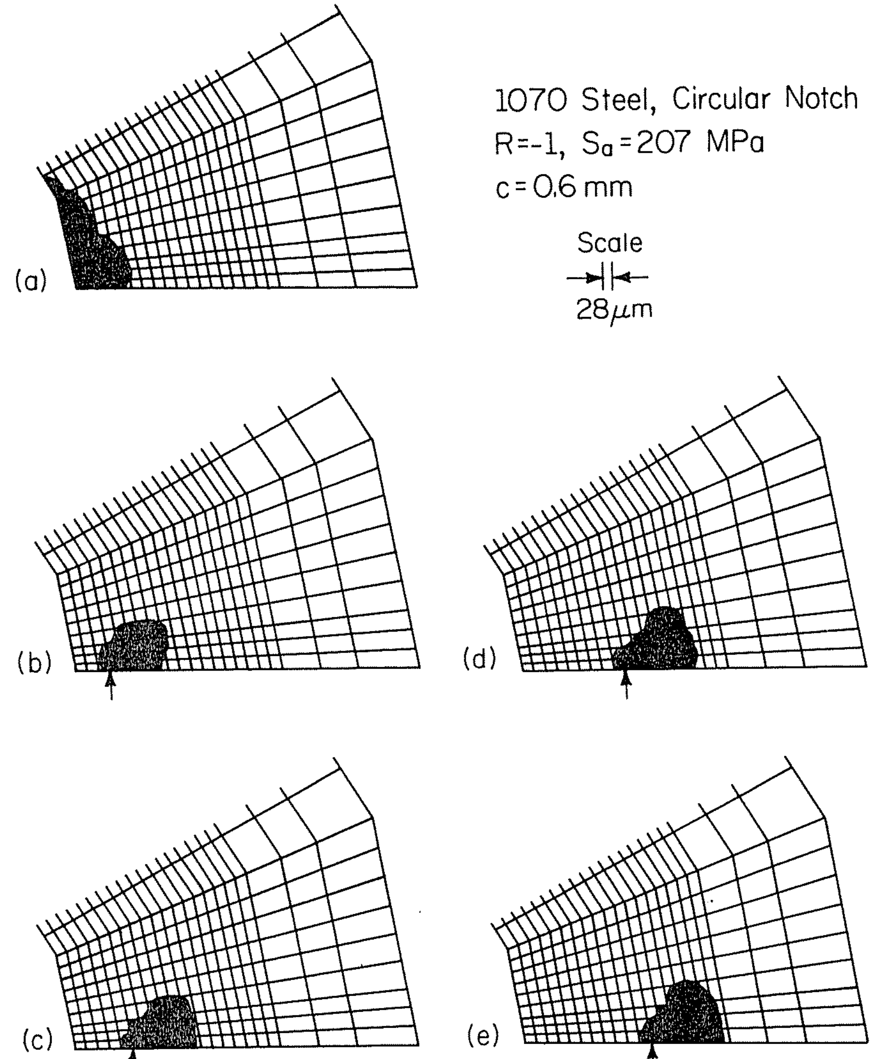

Fig 8 Notch and current crack tip plastic zone profiles at a maximum load for a series of crack lengths. Corresponding experimental crack growth rates are supplied below. Arrow indicates location of crack tip

(a) $l/c = 0.0$	
(b) $l/c = 0.138$	$da/dN = 1.77 \times 10^{-5}$ mm/cycle
(c) $l/c = 0.232$	$da/dN = 1.74 \times 10^{-5}$ mm/cycle
(d) $l/c = 0.418$	$da/dN = 1.62 \times 10^{-5}$ mm/cycle
(e) $l/c = 0.512$	$da/dN = 1.25 \times 10^{-5}$ mm/cycle

crack will be initially embedded in. A comparison of results is also made with the ABAQUS commercial FEM code. The present work uses a plasticity theory and constitutive law integration method similar to those in the ABAQUS code. The integration scheme is a mean normal, tangent stiffness method with radial return and subincrementation. For a discussion of these, refer to (**16**)–(**19**).

The notch plastic zone profile and crack tip plastic zone profile are shown for a series of crack lengths in Fig. 8. Examination of experimentally observed growth rates for this problem (Fig. 5) reveals the approximate crack length where growth rates reach a minimum value. This length appears to be at about $l/c = 0.60$ where c is half notch width. FEM results indicate the notch plastic zone to extend out to only about $l/c = 0.24$ for $S_a = 207$ MPa. Clearly, small crack behaviour continues at crack lengths well past the notch plastic zone size.

The ratio of the reversed crack tip plastic zone size, Δw, to the maximum crack tip plastic zone size, w, is influenced by the notch plastic zone as seen in Fig. 9. There exists a correspondence of this ratio with closure level (**2**). The opening and closure stresses increase with decreasing $\Delta w/w$ ratios. The rate of decrease in $\Delta w/w$ appears to be highest for $0 \geq l/c \geq r_p/c$ where r_p is the plastic zone of the notch.

The level of applied load also greatly influences crack closure behaviour for the $R = -1$ loading considered. Figure 10 is a plot of opening and closure levels versus normalized crack length for two different applied stress amplitudes. These results were generated with FEM. Although the opening and closure levels for $S_a = 310$ MPa have not been experimentally verified, the qualitative trends do agree with observed data (**20**). Both crack opening and closure levels are seen to be lower at higher applied stress amplitudes. Also note that the difference between crack closure level and opening level increases with higher applied stress amplitude. This has been observed experimentally (**20**).

Discussion of results

Experimental evidence (**2**)–(**4**)(**13**)–(**15**) has shown that physically small fatigue cracks grow at rates higher than expected based on the trends of long crack data. More specifically, in the notched member simulated here, growth rates for very small cracks were found to decrease to a minimum then increase with increasing crack length (Fig. 5). It has been proposed that crack closure may have a significant influence on the explanation of small crack growth behaviour. The FEM simulation described here accurately modeled the plastically deformed material ahead of a growing crack and thereby predicted crack opening and closure levels that are in good agreement with experimentally observed results.

The crack opening and closing levels increase progressively and then stabilize as the crack grows away from the notch (Fig. 4). Thus, the extent of closure appears to be related to physical crack size. The level of closure is strongly dictated by the material in the wake of the crack tip. In general, a smaller crack

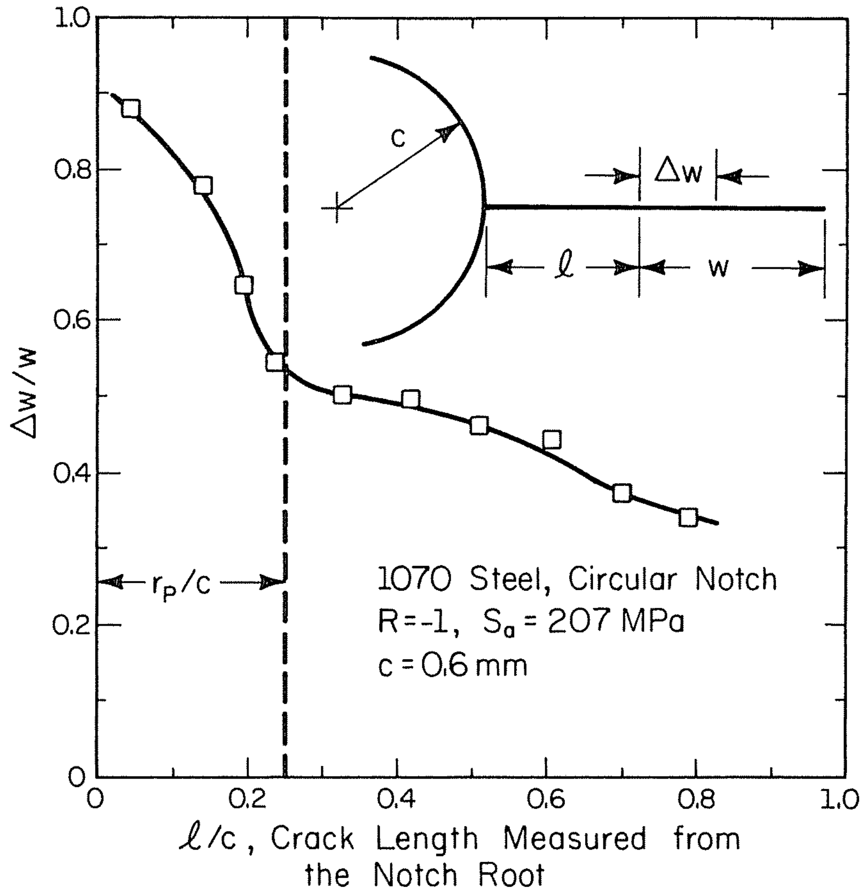

Fig 9 Ratio of reversed crack tip plastic zone to maximum crack tip plastic zone, $\Delta w/w$, for a crack growing from a circular notch

with a limited wake is less likely to experience closure effects than a long crack with a significant amount of plastically deformed material in its wake. Examining the stress fields for a relatively small and a long crack, Fig. 6(a) and 6(b), respectively, revealed that the longer crack has a larger region of compressive residual stresses that must be overcome by the applied load than that of the smaller crack. Since the small crack is embedded in the notch plastic zone, the magnitudes of the compressive residual stresses and the ensuing maximum tensile stresses for it are about the same as those for the longer crack. Therefore, the magnitude of these stresses seems less significant than the length of the wake in this argument.

It should be pointed out here that other factors also influence closure as

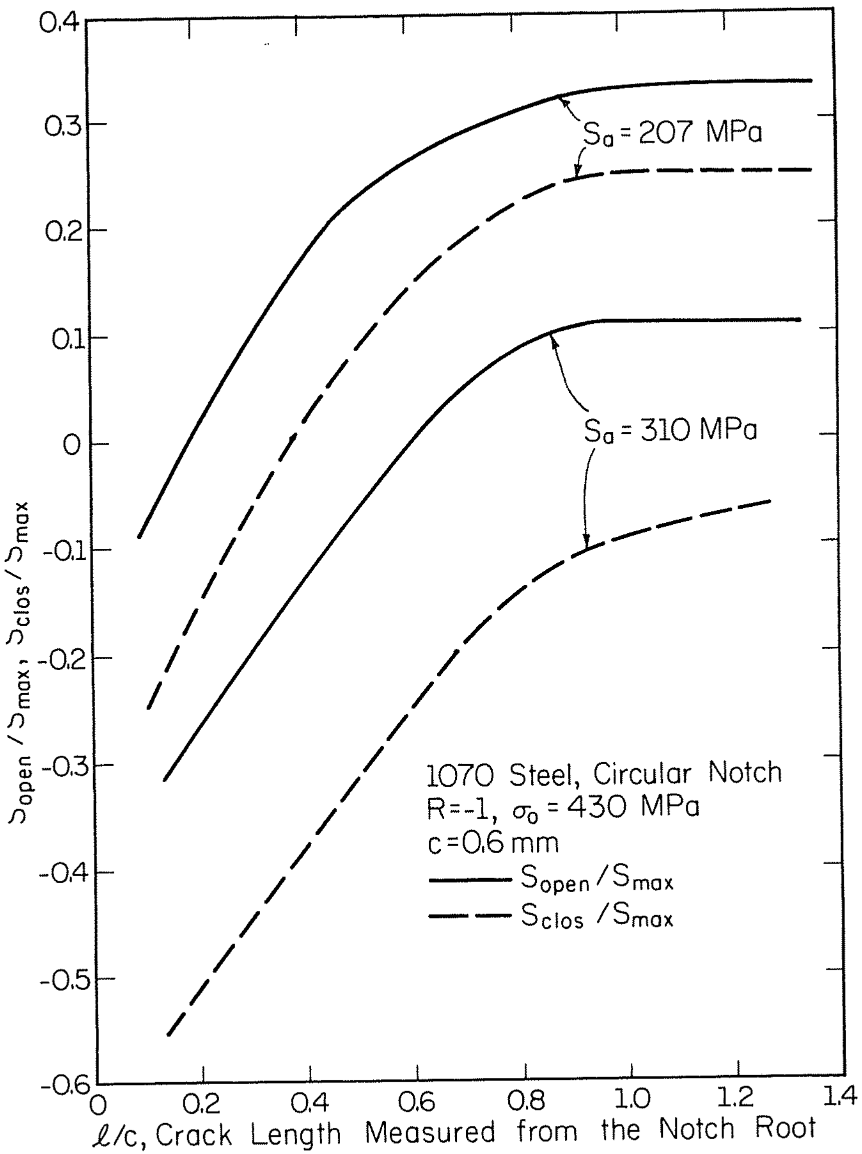

Fig 10 Influence of applied load level on crack opening and closure behaviour

experimental evidence in some studies did not observe closure levels to vary significantly with crack length (**20**). The effect of crack length on closure levels is more dominant for $R < 0$ than for $R \geq 0$ loading as indicated in other studies (**4**). Crack opening and closure levels were reported to be fairly independent of crack length for $R = 0$ in (**2**). This apparent lack of crack length influence may be explained by the results of an FEM analysis on the mesh in Fig. 1 run under $R = 0$ conditions. It was found that crack face contact did not extend completely behind the crack at minimum applied load for $R = 0$ loading for the same crack lengths considered. This is contrary to the $R = -1$ case. Therefore in the $R = 0$ case, the contact zone behind the crack for two different crack sizes may be equal, resulting in similar opening levels (**2**)(**21**).

Results of the numerical prediction of crack opening and closure levels can be applied to partly explain the anomalous propagation behaviour of small cracks. The ΔK_{eff} calculated over the range of crack lengths considered is illustrated in Fig. 5. Note the qualitative similitude between the dl/dN and ΔK_{eff} versus l/c curves. Since the extent of crack closure is minimal at small crack lengths (Fig. 4), the small cracks measured experience an initially high ΔK_{eff} that translates into a high growth rate. As the crack grows, the stress level required to open the crack allowing further propagation increases. This accounts for the decreasing growth rates. Eventually crack opening levels stabilize and one observes the small crack growth curve to merge with the long crack data.

Conclusions

A detailed simulation of a small fatigue crack growing from a notch has been carried out and results compare favourably with experiments. Admittedly, numerous factors thought to influence small crack behaviour have been omitted from the present analysis. Nevertheless the work supports some important conclusions.

(1) Crack closure levels for cracks emanating from blunt notches are a function of crack length for $R = -1$ loading. This dependency of crack closure level on crack length corresponds with observed propagation behaviour for both small and long cracks.

(2) Opening levels are consistently higher than closure levels for all crack lengths considered. This difference becomes more pronounced at higher applied stress amplitudes.

(3) Finite element method results correspond favourably with both experimental and analytical work. The FEM also provides other information (i.e., near crack stress fields and plastic zones for hardening material and for cyclic anisotropy) which can aid in the understanding of small crack behaviour.

(4) Crack opening and closure levels change with applied load level for $R = -1$ loading. The FEM satisfactorily predicts this dependence. Further work is needed in this area.

Acknowledgements

This research was funded by the Fracture Control Program, College of Engineering, University of Illinois at Urbana-Champaign.

References

(1) ELBER, W. (1971) The significance of fatigue crack closure, *Damage tolerance in aircraft structures, ASTM STP 486* (American Society for Testing and Materials), pp. 230–242.
(2) SEHITOGLU, H. (1985) Crack opening and closure in fatigue, *Engng Fracture Mech.*, **21**, 329–339.
(3) SEHITOGLU, H. (1985) Characterization of crack closure, *ASTM 16th Symposium on Fracture Mechanics, ASTM STP 868*, Colombus, Ohio (American Society for Testing and Materials), pp. 361–380.
(4) NEWMAN, J. C., Jr. (1982) A nonlinear fracture mechanics approach to growth of small cracks, Paper presented at the AGARD Meeting on Behaviour of Short Cracks in Airframe Components, Toronto, Canada.
(5) FUHRING, H. and SEEGER, T. (1979) Dugdale crack closure analysis of fatigue cracks under constant amplitude loading, *Engng Fracture Mech.*, **22**, 99–122.
(6) DILL, H. D. and SAFF, C. R. (1976) Spectrum crack growth prediction based on crack surface displacement and contact analysis, *ASTM STP 595* (American Society for Testing and Materials), pp. 306–319.
(7) DUGDALE, D. S. (1960) Yielding of steel sheet containing slits, *J. Mech. Phys. Solids*, **8**, 100–104.
(8) NEWMAN, J. C., Jr. (1976) A finite element analysis of fatigue crack closure, *Mechanics of Crack Growth, ASTM STP 590* (American Society for Testing and materials), pp. 281–301.
(9) SOCIE, D. F. (1973) Prediction of fatigue crack growth in notched members under variable amplitude loading histories, *Engng Fracture Mech.*, **9**, 849–865.
(10) OHJI, K., OGURA, K., and OHKUBA, Y. (1975) Cyclic analysis of a propagating crack and its correlation with fatigue crack growth, *Eng. Fracture Mech.*, **17**, 457–464.
(11) MORRIS, W. L., JAMES, M. R., and BUCK, O. (1981) Growth rate models for short surface cracks in Al 2219-T851, *Metall Trans*, **12A**, 57–64.
(12) ZIEGLER, H. (1959) A modification of Prager's hardening rule, *Q. Appl. Math.*, **XVII**, 55–65.
(13) SEHITOGLU, H. (1983) Fatigue life prediction of notched members based on local strain and elastic plastic fracture mechanics concepts, *Engng Fracture Mech.*, **18**, 609–621.
(14) HAMMOUDA, M. M., SMITH, R. A., and MILLER, K. J. Elastic–plastic fracture-mechanics for initiation and *R* of notch fatigue cracks, *Fatigue Engng Mater. Structures*, **2**, 139–154.
(15) HUDAK, S. J., Jr. (1981) Small crack behaviour and the prediction of fatigue life, *J. Engng Mater. Technol.*, **103**, 26–35.
(16) ABAQUS, *Theory Manual*, Version 4, 1982 (Hibbit, Karlson, and Sorenson, Providence, RI).
(17) RICE, J. R. and TRACEY, D. M. (1973) Computational fracture mechanics, *Numerical and computer methods in structural mechanics* (Edited by S. J. Fenves, N. Perrone, A. R. Robinson, and W. C. Schnobrich), (Academic Press, New York), pp. 585–623.
(18) KRIEG, R. D. and KRIEG, D. B. (1977) Accuracies of numerical solution methods for the elastic–perfectly plastic model, *J. Pressure Vessel Technol.*, **99**, 510–515.
(19) SCHREYER, H. L., KULAK, R. L., and KRAMER, J. M. (1979) Accurate numerical solutions for elastic–plastic models, *J. Pressure Vessel Technol.*, **101**, 226–234.
(20) McCLUNG, R. C. and SEHITOGLU, H. (1986) Closure behavior of short cracks under high strain fatigue histories, *Int. Symp. on Fatigue Crack Closure*, 1–2 May, Charleston, SC, USA.
(21) BUDIANSKY, B. and HUTCHINSON, J. W. (1978) Analysis of closure in fatigue crack growth, *J. Appl. Mech.*, **45**, 267–276.